

# SCIENTIFIC REPORTS



OPEN

## Lifespan Gyrfication Trajectories of Human Brain in Healthy Individuals and Patients with Major Psychiatric Disorders

Bo Cao<sup>1</sup>, Benson Mwangi<sup>1</sup>, Ives Cavalcante Passos<sup>2</sup>, Mon-Ju Wu<sup>1</sup>, Zafer Keser<sup>3</sup>, Giovana B. Zunta-Soares<sup>1</sup>, Dianping Xu<sup>1</sup>, Khader M. Hasan<sup>4</sup> & Jair C. Soares<sup>1</sup>

Cortical gyrfication of the brain represents the folding characteristic of the cerebral cortex. How the brain cortical gyrfication changes from childhood to old age in healthy human subjects is still unclear. Additionally, studies have shown regional gyrfication alterations in patients with major psychiatric disorders, such as major depressive disorder (MDD), bipolar disorder (BD), and schizophrenia (SCZ). However, whether the lifespan trajectory of gyrfication over the brain is altered in patients diagnosed with major psychiatric disorders is still unknown. In this study, we investigated the trajectories of gyrfication in three independent cohorts based on structural brain images of 881 subjects from age 4 to 83. We discovered that the trajectory of gyrfication during normal development and aging was not linear and could be modeled with a logarithmic function. We also found that the gyrfication trajectories of patients with MDD, BD and SCZ were deviated from the healthy one during adulthood, indicating altered aging in the brain of these patients.

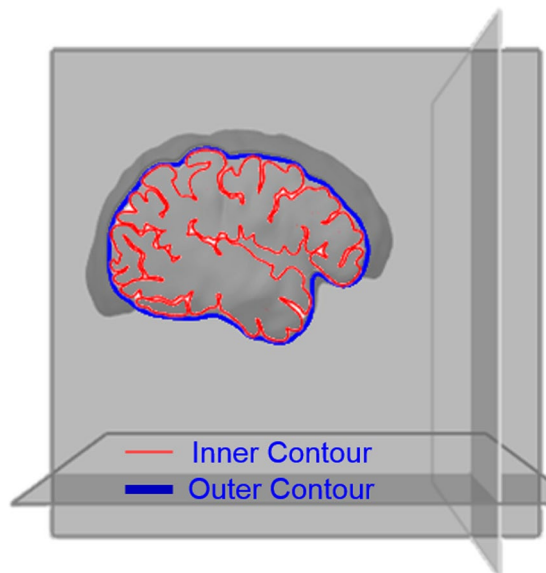
Cortical gyrfication of the brain represents the folding characteristic of the cerebral cortex, which increases the cortical surface area and thus the number of neurons in a limited cranium volume<sup>1</sup>. Cortical gyrfication can be represented with the gyrfication index (GI): a ratio of the total cortical inner surface area to the area of an outer surface that smoothly encloses the cortex<sup>2</sup> (Fig. 1). The GI increases with brain mass across species<sup>3</sup>, and GI decreases during healthy aging in humans<sup>4,5</sup>. The trajectory of brain cortical gyrfication from childhood to old age in human is still unknown. Additionally, it was hypothesized that major psychiatric disorders, such as major depressive disorder (MDD), bipolar disorder (BD), and schizophrenia (SCZ), are progressive disorders associated with altered development and aging<sup>6–13</sup>. This hypothesis is based on the association of these disorders with higher prevalence and earlier age of onset of age-related medical conditions<sup>14,15</sup> (e.g. cardiovascular diseases and dementia), earlier cognitive decline<sup>16</sup>, and shortened telomere length<sup>17</sup> compared to healthy controls (HC). It is possible therefore that the brain of patients with psychiatric disorders may also undergo abnormal changes during development and aging. Studies with small sample sizes have shown regional brain gyrfication alterations in patients with MDD<sup>18</sup>, BD<sup>19</sup> and SCZ<sup>20,21</sup>. However, it is still unknown whether the lifespan trajectories of gyrfication over the brain are altered in patients diagnosed with these psychiatric disorders and whether there are differential courses among them. In this study, we investigated the trajectory of gyrfication during normal development and aging in three independent cohorts. The gyrfication trajectory of healthy subjects made it possible for us to investigate the gyrfication trajectories of patients with MDD, BD and SCZ with a normative refs 22–25. We hypothesized that the gyrfication trajectories of patients with these major psychiatric disorders would deviate from that of the healthy subjects. Our results will fill the gap of our knowledge about the gyrfication trajectory over the lifespan and provide a dynamic perspective of understanding the brain alterations in psychiatric disorders.

<sup>1</sup>Department of Psychiatry and Behavioral Sciences, The University of Texas Health Science Center at Houston, Houston, Texas, USA. <sup>2</sup>Graduation Program in Psychiatry and Laboratory of Molecular Psychiatry, Federal University of Rio Grande do Sul, Porto Alegre, RS, Brazil. <sup>3</sup>Department of Neurology, The University of Texas Science Center at Houston, Houston, Texas, USA. <sup>4</sup>Department of Diagnostic and Interventional Imaging, The University of Texas Science Center at Houston, Houston, Texas, USA. Correspondence and requests for materials should be addressed to B.C. (email: [CloudBoCao@gmail.com](mailto:CloudBoCao@gmail.com))

Received: 22 November 2016

Accepted: 3 March 2017

Published online: 30 March 2017



$$GI = \frac{\text{Inner Contour Area}}{\text{Outer Contour Area}}$$

**Figure 1.** The illustration of cortical gyrification index (GI) as a ratio of the area of inner contour surface to the surface area of outer contour area.

Characteristic	HC (n = 510)	MDD (n = 95)	BD-I (n = 151)	SCZ (n = 125)	F/X <sup>2</sup>	P value
Sample						
SA	225	95	151	—		
NKI	139	—	—	—		
COBRE	146	—	—	125		
Age, y*					4.83	0.0024
SA	8–65 27.7 ± 14.2	9–62 36.5 ± 16.5	8–68 32.1 ± 16.1	—		
NKI	4–83 33.6 ± 20.1	—	—	19–64 38.4 ± 13.0		
COBRE	18–63 38.5 ± 11.5					
Gender**					15.32	<0.001
Male	57.5%(293)	36.8%(35)	45.0%(68)	78.4%(98)		
Female	42.5%(217)	63.2%(60)	55.0%(83)	21.6%(27)		

**Table 1.** Demographic information of all subjects. \*Mean and standard deviation, p value according to ANOVA; \*\*Relative (%) and absolute (n) frequencies; p value according to  $\chi^2$  test; Abbreviations: BD-I, Bipolar 1 Disorder; COBRE, Center of Biomedical Research Excellence; HC, Healthy Control; MDD, Major Depressive Disorder; NKI, Nathan Kline Institute; SA, San Antonio; SCZ, Schizophrenia.

## Results

The demographic information of the three independent cohorts is summarized in Table 1. In total, we have 510 HC, 95 patients with MDD, 151 patients with BD-I and 125 patients with SCZ, from age 4 to 83. The GI trajectory for HC was evaluated using the logarithmic function of age to fit the average GI trajectory (Eq. 1; see Materials and Methods), where  $a = 3.4000$ ,  $b = -0.1746$  and  $c = -2.9991$ . The coefficient of Pearson's correlation between the GI estimated by Eq. 1 and the whole brain GI for the HC from all the three cohorts was  $r = 0.75$  ( $p < 0.0001$ ), accounting for 56.4% of the total variance in the average GI of all HC. Specifically, the GI estimated by Eq. 1 could account for 53.8% ( $r = 0.73$ ;  $p < 0.0001$ ), 66.2% ( $r = 0.81$ ;  $p < 0.0001$ ) and 28.3% ( $r = 0.53$ ;  $p < 0.0001$ ) variance of SA, NKI and COBRE samples, respectively. The difference in the variance explained by the logarithmic function could at least partly be attributed to the individual differences within HC of each cohort, e.g., COBRE HC showed higher individual difference than the other two cohorts (Supplementary Materials Fig. S2). The gyrification

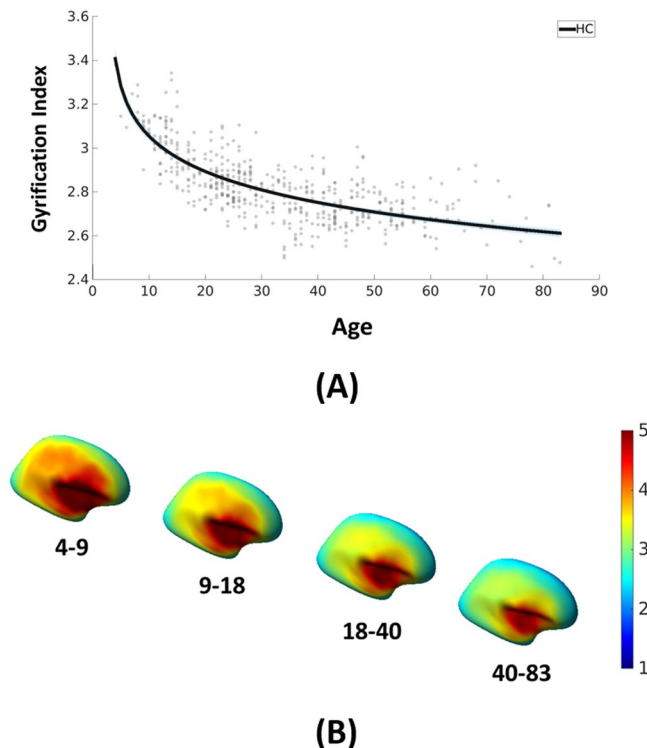


**Figure 2.** The gyrfication index trajectory during normal development and aging. **(A)** The non-linear gyrfication index trajectory for healthy subjects. The trajectory was well fitted with  $GI = a + b * \ln(\text{age} + c)$ , where  $a = 3.4000$ ,  $b = -0.1746$  and  $c = -2.9991$ . Note that the thin light gray area along the black line indicates the 95% fitting confidence of the trajectory. **(B)** Brain gyrfication changes over lifespan. Regional gyrfication was high in childhood and adolescence, but the decrease rate was also high during these periods. Overall gyrfication indices across the brain were low in adulthood, but the decrease rate was also low. The age ranges were chosen to best represent the gyrfication changes. Only lateral view is shown, because the gyrfication changes of medial regions over the lifespan was much less than the lateral regions (see Fig. S3). The colors represent the GI values.

indices across the brain decreased over the lifespan (Fig. 2B; Supplementary Materials Fig. S3). Regional brain gyrfication indices were generally higher during childhood and adolescence than adulthood, but the decrease rate was also more dramatic before adulthood.

The GI trajectories of patients with MDD, BD-I and SCZ were estimated individually with Eq. 1 (Fig. 3A). The GI estimated by Eq. 1 accounted for 54.8% ( $r = 0.74$ ;  $p < 0.0001$ ), 60.9% ( $r = 0.78$ ;  $p < 0.0001$ ) and 33.8% ( $r = 0.58$ ;  $p < 0.0001$ ) variance of MDD, BD-I and SCZ patients, respectively. BD-I ( $p = 0.0009$ ) and SCZ ( $p = 0.0427$ ) patients showed marked decrease of GI during adulthood, especially after the age of 40 (BD-I,  $p = 0.0021$ ; SCZ,  $p = 0.0004$ ), compared to HC (Fig. 3B).

To confirm the GI trajectories of patients with psychiatric disorders are different from the GI trajectory of healthy subjects, we estimated the parameters of Eq. 1 for each diagnosis group using resampling technique within each group. The fitting parameters,  $a$  and  $b$ , were not different across the HC in the three cohorts (Fig. S4). We found that the parameter  $a$  was lower than HC in MDD (Cohen's  $d = -1.68$ ;  $p < 0.0001$ ) and higher in BD-I (Cohen's  $d = 0.81$ ;  $p < 0.0001$ ) and SCZ (Cohen's  $d = 1.22$ ;  $p < 0.0001$ ), while the parameter  $b$ , which indicated the decrease rate of GI, was higher (less negative) than HC in MDD (Cohen's  $d = 1.66$ ;  $p < 0.0001$ ) and lower (more negative) in BD-I (Cohen's  $d = -1.35$ ;  $p < 0.0001$ ) and SCZ (Cohen's  $d = -1.48$ ;  $p < 0.0001$ ) than HC (Fig. 3C). These results showed that the GI of BD-I and SCZ decreased faster than HC during aging.

The gyrfication indices in multiple brain regions were significantly lower in the patients with BD-I and SCZ than HC during aging after the age of 40 (Fig. S6). No significant difference was found in MDD patients. The group-level comparison was performed at each vertex of the cortical surface. Only vertices with  $p$  values lower than the threshold  $p$  values obtained at a false discovery rate (FDR)<sup>26,27</sup> of 0.05 were shown. No further clustering adjustment was performed. To confirm the validity and uniformity of the combined HC sample, the HC of each of the three cohorts was compared to the combined HC sample, and no vertex was significantly different (Fig. S5). We also compared each of the patient samples to the corresponding HC sample within each cohort instead of the combined HC sample, and the results were similar to but less sensitive than the results with all HC (see Supplementary Materials Fig. S7).

## Discussion

To our best knowledge, this is the first *in vivo* study to show the cortical gyrfication index trajectory of the human brain over the lifespan, from age 4 to 83. During this age range, the GI trajectory follows a logarithmic function

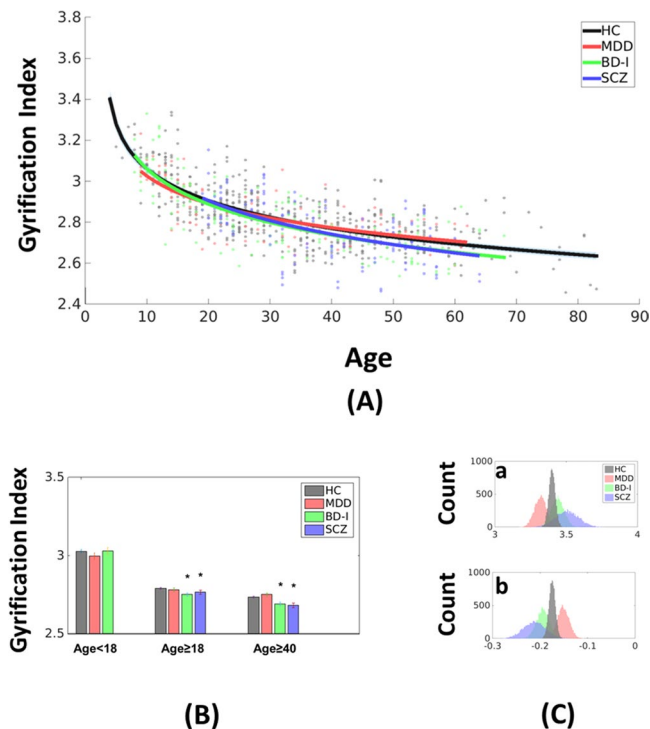


**Figure 3.** Abnormal gyrification trajectories in patients with major psychiatric disorders. **(A)** Patients with MDD, BD-I and SCZ showed deviated gyrification index (GI) trajectories from the trajectory of healthy subjects. Note that the thin light gray area along the black line indicates the 95% fitting confidence of the healthy trajectory. **(B)** The whole brain GI of healthy subjects and all the psychiatric groups in different age ranges. Patients with bipolar disorder and schizophrenia showed lower GI in the adulthood, especially after the age of 40. **(C)** Resampling results confirmed that the parameters of the fitting function for the GI trajectories of patients with psychiatric disorders were different from that of healthy subjects. Abbreviations: MDD, Major Depressive Disorder; BD-I, Bipolar 1 Disorder; SCZ, Schizophrenia; HC, healthy controls.

of age. This is an important advancement of our knowledge on human brain development and aging, as previous studies showed a linear decrease of GI during the adulthood<sup>4,28</sup>. Based on *post-mortem* studies, the gyrification increases after birth<sup>29,30</sup>, which was confirmed by a recent longitudinal imaging study on children before the age of two<sup>31</sup>. However, when the gyrification of human brain reaches its peak during development is still unknown. Although there have been studies suggesting that the brain complexity keeps increasing until teenage<sup>32</sup> and certain brain regions such as entorhinal cortex may have increased thickness until the age of 30<sup>33</sup>, our study suggests that the GI starts to decrease already around the age of four. The cellular mechanisms underlying the gyrification are still unclear<sup>34</sup>, although theories have been raised based on mechanical tension<sup>35</sup>, stress-dependent folding and differential growth<sup>36,37</sup>, regulated radial and tangential expansion<sup>38</sup>, axonal pushing<sup>39</sup> and minimization of effective free energy associated with cortical shape<sup>3,30</sup>. Most of these theories focused on the brain development during the young age, and the trajectory observed in the present study may be associated with different mechanisms. Thus, the gyrification trajectory established in this study will be valuable information that needs to be considered in the future gyrification theories considering both brain development and aging.

Our findings revealed abnormal gyrification trajectories in patients with major psychiatric disorders. The GI in patients with BD-I and SCZ decreased faster than HC during aging. The brain regions with altered gyrification indices in BD-I and SCZ are consistent with several previous brain imaging studies investigating them individually<sup>19,20,40,41</sup>. Patients with SCZ showed a significant decrease of GI in the dorsolateral prefrontal cortex, anterior cingulate cortex and supra-marginal cortex. The prefrontal cortex is known to be crucial for executive function<sup>42</sup> and working memory<sup>43</sup>. These important cognitive functions are impaired in SCZ<sup>44</sup>, which has been linked to the dysfunction of dorsolateral prefrontal cortex, such as low activity, low N-acetylaspartate concentration and abnormal dopamine metabolisms<sup>45–47</sup>. The anterior cingulate cortex is the key region for conflict monitoring, motivation modulation and mood regulation<sup>48–50</sup>, the pathology of which has been shown in mood disorders and schizophrenia<sup>51–54</sup>. The abnormally decreased gyrification indices of these regions are in line with the altered cognitive monitoring and executive control<sup>55</sup> in SCZ. The GI decrease in patients with BD-I was less extensive compared to patients with SCZ. However, lower GI in BD-I than HC in inferior frontal regions was consistent with previous studies on cortical gray matters<sup>56</sup>. We also found that the gyrification trajectory of patients with MDD might be different from HC, as well as from BD-I and SCZ, but no brain region showed significant alteration of gyrification in MDD. In fact, several studies with small sample size showed higher gyrification in MDD than in healthy controls<sup>57,58</sup>, while some showed lower<sup>18,59</sup>, which could be due to differences in genes or brain connections<sup>57,59</sup>. Further studies will be necessary to clarify these inconsistent results. However, our results did show a

possible decrease of gyrification index in MDD at a young age, which can be confirmed with future longitudinal studies focusing on pediatric MDD. The more significant decrease of gyrification in BD and SCZ compared to MDD could also be related to the possible damages due to manic episodes in BD and positive symptoms in SCZ indicated in the neuroprogression theory of BD and SCZ<sup>60,61</sup>. In addition, this is in line with recent studies, which suggested that the number of manic episodes seems to be the clinical marker more robustly associated with brain changes and neuroprogression in BD<sup>61</sup>. Given that the psychiatric disorders have been a major burden<sup>62</sup> in this aging world<sup>63</sup>, brain markers of abnormal aging, such as the gyrification index, may help us understand the mechanisms of brain aging, evaluate future strategies to slow down the degenerative process and relieve the burden caused by these major psychiatric disorders.

Some limitations should be considered in our study. The GI trajectory over the lifespan was developed using only cross-sectional data, and longitudinal data with multiple follow-ups were necessary to map the individual GI trajectory and to compare the individual differences of the GI trajectory during aging. The GI obtained with the automated algorithm was slightly higher than the ones in the previous studies<sup>31,64</sup>. However, a recent study showed a similar range of GI using the same automated algorithm<sup>65</sup>. Our study covered a large age range of human lifespan from 4 to 83, but the GI trajectory before the age of four was not included. This was due to multiple limitations, e.g., the data that were publicly available over the lifespan usually did not include children below the age of four; there were challenges to perform MRI scans on young children due to the head motion; and validation of the current automated algorithm on young children was still necessary.

In summary, the present study demonstrated for the first time that the gyrification of the human brain *in vivo* decreased non-linearly from the age of 4 to 83 and this process could be modeled with a logarithmic function of age. The results were consistent across three independent cohorts. Moreover, by comparing the gyrification trajectories of healthy subjects and patients diagnosed with major psychiatric disorders, such as major depressive disorder, bipolar disorder, and schizophrenia, we provided consistent evidence that these disorders were associated with abnormal gyrification during aging. These results will advance our knowledge about how our brain changes during normal and abnormal aging.

## Materials and Methods

**Samples.** Structural brain images from 881 subjects were collected with T1-weighted magnetic resonance imaging (MRI) from three independent cohorts: a sample collected at San Antonio (the SA sample), a sample collected at Nathan Kline Institute - Rockland (the NKI sample)<sup>66</sup> and a sample collected by the Centers of Biomedical Research Excellence (the COBRE sample). The latter two samples were publicly available. All patients completed the Structured Clinical Interview for DSM-IV Axis I Disorders (SCID) and met the corresponding DSM-IV criteria for MDD, bipolar 1 disorder (BD-I) or SCZ. Healthy controls (HC) had no current condition or history of psychiatric dysfunctions. All subjects had no history of neurological diseases. Signed informed consent have been obtained from all the subjects. No identifiable image from a specific subject was used for publication. The study protocols were approved by the Institutional Review Boards at the University of Texas at San Antonio in accordance with their guidelines and regulations.

**Image Acquisition and Processing.** The SA sample was all acquired at one Philips 1.5 Tesla MRI scanner (Philips Medical System, Andover, MA, USA) with a three-dimensional axial fast field echo sequence with the following parameters: repetition time (TR) = 24 ms, echo time (TE) = 5 ms, flip angle = 40°, field of view (FOV) = 256 mm, slice thickness = 1 mm, matrix size = 256 × 256 and 150 slices. All scans were visually inspected to rule out gross artifacts. The NKI sample was acquired at one 3 Tesla Siemens Magnetom TrioTim syngo scanner with a three-dimensional magnetization-prepared radio-frequency pulses and rapid gradient-echo (MPRAGE) sequence with the following parameters: TR = 2500 ms, TE = 3.5 ms, flip angle = 8°, FOV = 256 mm, slice thickness = 1 mm, matrix size = 256 × 256 and 192 slices (see [http://fcon\\_1000.projects.nitrc.org/indi/pro/nki.html](http://fcon_1000.projects.nitrc.org/indi/pro/nki.html)). The COBRE sample was acquired at one 3 Tesla Siemens Magnetom TrioTim syngo scanner with a three-dimensional multi-echo (ME-MPRAGE) sequence with the following parameters: TR = 2530 ms, TE = 1.64, 3.5, 5.36, 7.22, 9.08 ms, flip angle = 7°, FOV = 256 mm, slice thickness = 1 mm, matrix size = 256 × 256 and 176 slices (see [http://fcon\\_1000.projects.nitrc.org/indi/retro/cobre.html](http://fcon_1000.projects.nitrc.org/indi/retro/cobre.html)).

The structural brain images were preprocessed and the cortical surface of each brain was reconstructed with Freesurfer<sup>67,68</sup> (version 5.3, <http://surfer.nmr.mgh.harvard.edu/>). The reconstructed images were visually inspected by the authors to exclude the apparent reconstruction errors. The local gyrification index (GI) at each vertex of the reconstructed cortical surface mesh was calculated using the toolbox in Freesurfer with default settings<sup>69</sup>. Briefly, a circular region of interest was delineated on the outer surface, and its corresponding region of interest on the inner cortical surface was identified using a matching algorithm as described elsewhere<sup>70</sup> and the ratio between the folded inner cortical surface and its corresponding exposed outer surface was calculated as GI. The resulted GI values of each subject were smoothly sampled (Gaussian kernel, 10 mm) onto an average template provided by Freesurfer (fsaverage; 163842 vertices), so that cross individual comparison could be performed. The averaged GI for each subject was also calculated to represent the gyrification of whole brain.

The effect of brain volume on GI was taken into account for by adjusting the GI values with a linear regression of intracranial volume (ICV) on GI at each vertex and the whole brain GI, because previous studies found that the GI could be correlated with the brain volume<sup>31,71</sup>.

**Modeling Gyrification Trajectory as a function of Age.** We compared the fitting of the whole brain GI with age from ten common mathematical functions and chose the best function based on the averaged mean squared errors (MSE). The MSE of each fitting function was calculated with the non-linear fitting functions of the Statistics and Machine Learning Toolbox in MATLAB (The MathWorks, Inc., Natick, Massachusetts, United States) using default settings. Because the COBRE sample only included adults, it was not involved in the function

selection process. For SA and NKI samples, the MSE of each function was calculated based on the residuals derived from two types of validation procedures: (a) a leave-one-out cross-validation within each of the two samples and (b) a cross-sample validation, in which a fitting function was optimized for one sample and tested on the other. Thus, we had four MSEs for each function and the averaged of these MSEs was used as the fitting performance for the corresponding function as shown in Table S1. The best function was the logarithmic function with three parameters.

As a result, we used the following logarithmic function of age to fit the average GI trajectory:

$$GI = a + b * \ln(\text{age} + c) \quad (1)$$

where  $a$  was an indicator of GI levels independent of age,  $b$  controlled the decrease rate of GI over age and  $c$  was the translational term of age. The initial value of  $a$  was set to 4, because the mean of the brain average GI values of all the HC subjects was around 3 and the maximum whole brain GI was near 4. The initial value of  $b$  was set to  $-1$ , because GI apparently decreased with age. The initial value of  $c$  was set to 0. We found that  $c$  was sensitive to the age range of the sample and we had varied age range in COBRE HC, MDD, BD and SCZ samples. Furthermore,  $c$  did not provide any information of the GI levels and trajectory shapes, and its value was consistent in SA and NKI HC samples. In order to reliably compare the GI trajectories of all the samples without changing the shape and levels of GI trajectory, we fixed the  $c$  value to  $-2.9991$  according to the cross-validated fitting for the combined SA and NKI HC sample. Then each of the MDD, BD and SCZ groups was fitted separately.

GI was adjusted for study site by an amount of the estimated GI difference between the HC in each cohort and the combined SA and NKI HC sample at a given age  $[a_{HC} + b_{HC} * \ln(\text{age} + c)] - [a_X + b_X * \ln(\text{age} + c)]$ , where X represents the sample of HC in SA, NKI and COBRE cohorts and the mean adjustment values were as small as  $-0.0023$ ,  $0.0043$  and  $0.0523$ , respectively. The adjustment for the COBRE HC was larger than the other two cohorts, because the GI in the COBRE HC sample was generally lower than the HC in the other two cohorts, which could also be observed in the mean GI of adult HC in the COBRE cohort (2.748) compared to the GI of adult HC in SA (2.7938) and NKI cohorts (2.7777). To further confirm whether the adjustment introduced significant effect in the SCZ sample in the COBRE cohort, we also compared the GI over the brain of HC and SCZ within the COBRE cohorts.

Although the samples showed different distributions of males and females (see also<sup>72</sup>), which might have an effect on the GI trajectory of the samples with major psychiatric disorders, we found that effect of gender on GI was negligible after GI was adjusted by the ICV (Supplementary Materials Fig. S1). This might indicate that the gender effect on GI could be mostly explained by the brain volume. Thus, no further adjustment for gender was performed.

**Estimating the Parameters with Resampling.** In order to quantify the difference between the GI trajectories of HC, MDD, BD-I and SCZ, it was necessary to estimate the distributions of fitting parameters. We utilized the resampling technique. Briefly, for each of the HC, MDD, BD and SCZ samples, the sample was re-sampled 10000 times and the fitting was performed for each of the 10000 samples. In order to stratify the age distribution during the resampling, each sample was divided into four age blocks: 4–9, 9–18, 18–40 and 40–83. During each iteration of the resampling, 50% of the subjects in each age block were selected without duplicate. Thus, we had 10000 sets of parameters for each sample, and it was then possible to estimate the distributions of the fitting parameters in different samples.

## References

- Rakic, P. Evolution of the neocortex: a perspective from developmental biology. *Nat. Rev. Neurosci.* **10**, 724–35 (2009).
- Zilles, K., Armstrong, E., Schleicher, A. & Kretschmann, H. The human pattern of gyrification in the cerebral cortex. *Anat. Embryol. (Berl)*. **179**, 173–179 (1988).
- Mota, B. & Herculano-Houzel, S. Cortical folding scales universally with surface area and thickness, not number of neurons. *Science* **349**, 74–7 (2015).
- Hogstrom, L. J., Westlye, L. T., Walhovd, K. B. & Fjell, A. M. The structure of the cerebral cortex across adult life: Age-related patterns of surface area, thickness, and gyrification. *Cereb. Cortex* **23**, 2521–2530 (2013).
- Jockwitz, C. *et al.* Age- and function-related regional changes in cortical folding of the default mode network in older adults. *Brain Struct. Funct.* doi:10.1007/s00429-016-1202-4 (2016).
- Verhoeven, J. E. *et al.* Major depressive disorder and accelerated cellular aging: results from a large psychiatric cohort study. *Mol. Psychiatry* 1–7, doi:10.1038/mp.2013.151 (2014).
- Rizzo, L. B. *et al.* The theory of bipolar disorder as an illness of accelerated aging: Implications for clinical care and research. *Neurosci. Biobehav. Rev.* **42**, 157–169 (2014).
- Schnack, H. G. *et al.* Accelerated Brain Aging in Schizophrenia: A Longitudinal Pattern Recognition Study. *Am. J. Psychiatry* appiajpp201515070922, doi:10.1176/appi.ajp.2015.15070922 (2016).
- Cao, B. *et al.* Hippocampal volume and verbal memory performance in late-stage bipolar disorder. *J. Psychiatr. Res.* **73**, 102–7 (2016).
- Lavagnino, L. *et al.* Changes in the corpus callosum in women with late-stage bipolar disorder. *Acta Psychiatr. Scand.* **131**, 458–64 (2015).
- Cao, B., Passos, I. C., Mwangi, B., Amaral-Silva, H., Tannous, J., Wu, M. J., Zunta-Soares, G. B. & Soares, J. C. Hippocampal subfield volumes in mood disorders. *Molecular Psychiatry* doi:10.1038/mp.2016.262 (2017).
- Cao, B., Stanley, J. A., Passos, I. C., Mwangi, B., Selvaraj, S., Zunta-Soares, G. B. & Soares, J. C. Elevated Choline-Containing Compound Levels in Rapid Cycling Bipolar Disorder. *Neuropsychopharmacology* doi:10.1038/npp.2017.39 (2017).
- Passos, I. C., Mwangi, B., Vieta, E., Berk, M. & Kapczinski, F. Areas of controversy in neuroprogression in bipolar disorder. *Acta Psychiatr. Scand.* **134**(2), 91–103, doi:10.1111/acps.12581 (2016).
- da Silva, J., Gonçalves-Pereira, M., Xavier, M. & Mukaetova-Ladinska, E. B. Affective disorders and risk of developing dementia: systematic review. *Br. J. Psychiatry* **202**, 177–86 (2013).
- Crump, C., Sundquist, K., Winkleby, M. A. & Sundquist, J. Comorbidities and mortality in bipolar disorder: a Swedish national cohort study. *JAMA psychiatry* **70**, 931–9 (2013).
- Berk, M. *et al.* Pathways underlying neuroprogression in bipolar disorder: focus on inflammation, oxidative stress and neurotrophic factors. *Neurosci. Biobehav. Rev.* **35**, 804–17 (2011).

17. Lindqvist, D. *et al.* Psychiatric disorders and leukocyte telomere length: Underlying mechanisms linking mental illness with cellular aging. *Neurosci. Biobehav. Rev.* **55**, 333–64 (2015).
18. Zhang, Y., Yu, C., Zhou, Y. & Li, K. Decreased gyrification in major depressive disorder. *Neuroreport* 378–380, doi:10.1097/WNR.0b013e3283249b34 (2009).
19. McIntosh, A. M. *et al.* Prefrontal gyral folding and its cognitive correlates in bipolar disorder and schizophrenia. *Acta Psychiatr. Scand* **119**, 192–8 (2009).
20. White, T., Andreasen, N. C., Nopoulos, P. & Magnotta, V. Gyrification abnormalities in childhood- and adolescent-onset schizophrenia. *Biol. Psychiatry* **54**, 418–426 (2003).
21. Bonnici, H. M. *et al.* Pre-frontal lobe gyrification index in schizophrenia, mental retardation and comorbid groups: An automated study. *Neuroimage* **35**, 648–654 (2007).
22. Cao, B. *et al.* Development and validation of a brain maturation index using longitudinal neuroanatomical scans. *Neuroimage* **117**, 311–318 (2015).
23. Douaud, G. *et al.* Schizophrenia delays and alters maturation of the brain in adolescence. *Brain* **132**, 2437–2448 (2009).
24. Gur, R. C. *et al.* Neurocognitive growth charting in psychosis spectrum youths. *JAMA psychiatry* **71**, 366–74 (2014).
25. Dosenbach, N. U. F. *et al.* Prediction of individual brain maturity using fMRI. *Science* **329**, 1358–1361 (2010).
26. Benjamini, Y. & Hochberg, Y. Controlling the false discovery rate: a practical and powerful approach to multiple testing. *J. R. Stat. Soc. Ser. B* ... **57**, 289–300 (1995).
27. Nichols, T. & Hayasaka, S. Controlling the familywise error rate in functional neuroimaging: a comparative review. *Stat. Methods Med. Res.* **12**, 419–446 (2003).
28. Magnotta, V. A. *et al.* Quantitative *in vivo* measurement of gyrification in the human brain: changes associated with aging. *Cereb Cortex* **9**, 151–160 (1999).
29. Armstrong, E. *et al.* The ontogeny of human gyrification. *Cereb. cortex* **5**, 56–63 (1995).
30. Zilles, K., Palomero-Gallagher, N. & Amunts, K. Development of cortical folding during evolution and ontogeny. *Trends in Neurosciences* **36**, 275–284 (2013).
31. Li, G. *et al.* Mapping Longitudinal Development of Local Cortical Gyrification in Infants from Birth to 2 Years of Age. *J. Neurosci.* **34**, 4228–4238 (2014).
32. Blanton, R. E. *et al.* Mapping cortical asymmetry and complexity patterns in normal children. *Psychiatry Res. - Neuroimaging* **107**, 29–43 (2001).
33. Hasan, K. M. *et al.* Entorhinal Cortex Thickness across the Human Lifespan. *J. Neuroimaging* doi:10.1111/jon.12297 (2015).
34. Ronan, L. & Fletcher, P. C. From genes to folds: a review of cortical gyrification theory. *Brain Struct. Funct.* **220**, 2475–2483 (2015).
35. Van Essen, D. C. A tension-based theory of morphogenesis and compact wiring in the central nervous system. *Nature* **385**, 313–318 (1997).
36. Xu, G. *et al.* Axons Pull on the Brain, But Tension Does Not Drive Cortical Folding. *J. Biomech. Eng.* **132**, 071013 (2010).
37. Bayly, P. V. *et al.* A cortical folding model incorporating stress-dependent growth explains gyral wavelengths and stress patterns in the developing brain. *Phys. Biol.* **10**, 016005 (2013).
38. Stahl, R. *et al.* Trnp1 Regulates Expansion and Folding of the Mammalian Cerebral Cortex by Control of Radial Glial Fate. *Cell* **153**, 535–549 (2013).
39. Nie, J. *et al.* Axonal fiber terminations concentrate on gyri. *Cereb. Cortex* **22**, 2831–9 (2012).
40. Palaniyappan, L., Mallikarjun, P., Joseph, V., White, T. P. & Liddle, P. F. Folding of the prefrontal cortex in schizophrenia: Regional differences in gyrification. *Biol. Psychiatry* **69**, 974–979 (2011).
41. Mwangi, B. *et al.* Individualized Prediction and Clinical Staging of Bipolar Disorders Using Neuroanatomical Biomarkers. *Biol. Psychiatry Cogn. Neurosci. Neuroimaging* **1**, 186–194 (2016).
42. Elliott, R. Executive functions and their disorders. *Br. Med. Bull.* **65**, 49–59 (2003).
43. Goldman-Rakic, P. Cellular basis of working memory. *Neuron* **14**, 477–485 (1995).
44. Weinberger, D. R. & Gallhofer, B. Cognitive function in schizophrenia. *Int. Clin. Psychopharmacol.* **12** Suppl 4, S29–36 (1997).
45. Callicott, J. H. *et al.* Physiological Dysfunction of the Dorsolateral Prefrontal Cortex in Schizophrenia Revisited. *Cereb. Cortex* **10**, 1078–1092 (2000).
46. Brozoski, T. J., Brown, R. M., Rosvold, H. E. & Goldman, P. S. Cognitive deficit caused by regional depletion of dopamine in prefrontal cortex of rhesus monkey. *Science* **205**, 929–32 (1979).
47. Weinberger, D. R., Berman, K. F. & Zec, R. F. Physiologic dysfunction of dorsolateral prefrontal cortex in schizophrenia. I. Regional cerebral blood flow evidence. *Arch. Gen. Psychiatry* **43**, 114–124 (1986).
48. Bush, G., Luu, P. & Posner, M. Cognitive and emotional influences in anterior cingulate cortex. *Trends Cogn. Sci.* **4**, 215–222 (2000).
49. Amiez, C., Joseph, J. P. & Procyk, E. Reward encoding in the monkey anterior cingulate cortex. *Cereb. Cortex* **16**, 1040–55 (2006).
50. Carter, C. S. *et al.* Anterior cingulate cortex, error detection, and the online monitoring of performance. *Science* **280**, 747–9 (1998).
51. Dolan, R. J. *et al.* Dopaminergic modulation of impaired cognitive activation in the anterior cingulate cortex in schizophrenia. *Nature* **378**, 180–182 (1995).
52. Drevets, W. C. *et al.* Subgenual prefrontal cortex abnormalities in mood disorders. *Nature* **386**, 824–827 (1997).
53. Schmaal, L. *et al.* Cortical abnormalities in adults and adolescents with major depression based on brain scans from 20 cohorts worldwide in the ENIGMA Major Depressive Disorder Working Group. *Mol. Psychiatry* doi:10.1038/mp.2016.60 (2016).
54. Cao, B. *et al.* Evidence of altered membrane phospholipid metabolism in the anterior cingulate cortex and striatum of patients with bipolar disorder I: A multi-voxel 1H MRS study. *J. Psychiatr. Res.* **81**, 48–55 (2016).
55. MacDonald, A. W. *et al.* Dissociating the role of the dorsolateral prefrontal and anterior cingulate cortex in cognitive control. *Science* **288**, 1835–8 (2000).
56. Mwangi, B. *et al.* Individualized Prediction and Clinical Staging of Bipolar Disorders Using Neuroanatomical Biomarkers. *Biol. Psychiatry Cogn. Neurosci. Neuroimaging* **1**, 186–194 (2016).
57. Han, K.-M. *et al.* Local gyrification index in patients with major depressive disorder and its association with tryptophan hydroxylase-2 (TPH2) polymorphism. *Hum. Brain Mapp.* doi:10.1002/hbm.23455 (2016).
58. Peng, D. *et al.* Surface Vulnerability of Cerebral Cortex to Major Depressive Disorder. *PLoS One* **10**, e0120704 (2015).
59. Nixon, N. L. *et al.* Biological vulnerability to depression: linked structural and functional brain network findings. *Br. J. Psychiatry* **204**, 283–289 (2014).
60. Andreasen, N. C. *et al.* Progressive brain change in schizophrenia: a prospective longitudinal study of first-episode schizophrenia. *Biol. Psychiatry* **70**, 672–9 (2011).
61. Passos, I. C., Mwangi, B., Vieta, E., Berk, M. & Kapczinski, F. Areas of controversy in neuroprogression in bipolar disorder. *Acta Psychiatr. Scand.* **134**, 91–103 (2016).
62. Whiteford, H. A. *et al.* Global burden of disease attributable to mental and substance use disorders: Findings from the Global Burden of Disease Study 2010. *Lancet* **382**, 1575–1586 (2013).
63. He, W., Goodkind, D. & Kowal, P. An Aging World: 2015 International Population Reports. *United States Census Bur.* 204, doi:P95/09-1 (2016).
64. Raznahan, A. *et al.* How does your cortex grow? *J. Neurosci.* **31**, 7174–7177 (2011).
65. Gregory, M. D. *et al.* Regional Variations in Brain Gyrification Are Associated with General Cognitive Ability in Humans. *Curr. Biol.* **26**, 1301–1305 (2015).

66. Nooner, K. B. *et al.* The NKI-Rockland sample: A model for accelerating the pace of discovery science in psychiatry. *Frontiers in Neuroscience*. doi:[10.3389/fnins.2012.00152](https://doi.org/10.3389/fnins.2012.00152) (2012).
67. Fischl, B., Sereno, M. I. & Dale, A. M. Cortical surface-based analysis. II: Inflation, flattening, and a surface-based coordinate system. *Neuroimage* **9**, 195–207 (1999).
68. Dale, A. M., Fischl, B. & Sereno, M. I. Cortical surface-based analysis. I. Segmentation and surface reconstruction. *Neuroimage* **9**, 179–194 (1999).
69. Schaer, M. *et al.* How to Measure Cortical Folding from MR Images: a Step-by-Step Tutorial to Compute Local Gyrification Index. *J. Vis. Exp.* 1–8, doi:[10.3791/3417](https://doi.org/10.3791/3417) (2012).
70. Schaer, M. *et al.* A Surface-based approach to quantify local cortical gyrification. *IEEE Trans. Med. Imaging* **27**, 161–170 (2008).
71. Toro, R. *et al.* Brain size and folding of the human cerebral cortex. *Cereb. Cortex* **18**, 2352–2357 (2008).
72. Gregory, M. D. *et al.* Regional Variations in Brain Gyrification Are Associated with General Cognitive Ability in Humans. *Curr. Biol.* **26**, 1301–1305 (2015).

## Acknowledgements

Supported in part by NIMH grant R01 085667, the Dunn Research Foundation and the Pat Rutherford, Jr. Endowed Chair in Psychiatry (Jair C. Soares) and NARSAD Young Investigator Grants of The Brain & Behavior Research Foundation (Bo Cao). The COBRE cohorts was collected in the support of NIH COBRE Grant No. P20 RR021938, and was processed with a server in the personal financial support from Dianping Xu.

## Author Contributions

Dr. Cao designed the study, processed and analyzed the data from all cohorts, drafted the manuscript, and critically edited the draft of the manuscript. Dr. Mwangi was involved in designing the study, partly processed the SA and NKI data, and critically edited the draft of the manuscript. Dr. Passos partly drafted the manuscript, and critically edited the draft of the manuscript. Dr. Wu partly processed the SA data and critically edited the draft of the manuscript. Dr. Keser critically edited the draft of the manuscript. Dr. Zunta-Soares coordinated the subject enrollment and data collection in the SA cohort. Mrs. Xu provided financial support for processing the COBRE cohort and critically edited the draft of the manuscript. Dr. Hasan was involved in designing the study, and critically edited the draft of the manuscript. Dr. Soares supervised the study, provided financial and instrumental support, collected the data of the SA cohort, and critically edited the draft of the manuscript.

## Additional Information

**Supplementary information** accompanies this paper at doi:[10.1038/s41598-017-00582-1](https://doi.org/10.1038/s41598-017-00582-1)

**Competing Interests:** Dr. Cao, Dr. Mwangi, Dr. Passos, Dr. Wu, Dr. Keser, Dr. Zunta-Soares, Mrs. Xu and Dr. Hasan reported no biomedical financial interests or potential conflicts of interest. Dr. Soares has received grants/research support from Forrest, BMS, J&J, Merck, Stanley Medical Research Institute, NIH and has been a speaker for Pfizer and Abbott.

**Publisher's note:** Springer Nature remains neutral with regard to jurisdictional claims in published maps and institutional affiliations.



**Open Access** This article is licensed under a Creative Commons Attribution 4.0 International License, which permits use, sharing, adaptation, distribution and reproduction in any medium or format, as long as you give appropriate credit to the original author(s) and the source, provide a link to the Creative Commons license, and indicate if changes were made. The images or other third party material in this article are included in the article's Creative Commons license, unless indicated otherwise in a credit line to the material. If material is not included in the article's Creative Commons license and your intended use is not permitted by statutory regulation or exceeds the permitted use, you will need to obtain permission directly from the copyright holder. To view a copy of this license, visit <http://creativecommons.org/licenses/by/4.0/>.

© The Author(s) 2017